

**Original contribution**

Myoepithelial cells in lobular carcinoma in situ: distribution and immunophenotype ^{☆, ☆ ☆}



Ying Wang MD, PhD^a, Sonali Jindal MD^b, Maritza Martel MD^c, Yaping Wu MD^c,
Pepper Schedin PhD^{b,d}, Megan Troxell MD, PhD^{a,d,*}

^aDepartment of Pathology, Oregon Health & Science University, Portland, OR 97239

^bDepartment of Cell, Developmental and Cancer Biology, Oregon Health & Science University, Portland, OR 97239

^cDepartment of Pathology, Providence Health and Services, Portland, OR 97213

^dOregon Health & Science University, Knight Cancer Institute, Portland, OR 97239

Received 8 February 2016; revised 15 April 2016; accepted 5 May 2016

Keywords:

Lobular carcinoma in situ (LCIS);
Myoepithelial cell;
Immunohistochemistry p63;
Smooth muscle myosin heavy chain;
Calponin;
Smooth muscle actin

Summary Myoepithelial cells have important physical and paracrine roles in breast tissue development, maintenance, and tumor suppression. Recent molecular and immunohistochemical studies have demonstrated phenotypic alterations in ductal carcinoma in situ–associated myoepithelial cells. Although the relationship of lobular carcinoma in situ (LCIS) and myoepithelial cells was described in 1980, further characterization of LCIS-associated myoepithelial cells is lacking. We stained 27 breast specimens harboring abundant LCIS with antibodies to smooth muscle myosin heavy chain, smooth muscle actin, and calponin. Dual stains for E-cadherin/smooth muscle myosin heavy chain and CK7/p63 were also performed. In each case, the intensity and distribution of staining in LCIS-associated myoepithelial cells were compared with normal breast tissue on the same slide. In 78% of the cases, LCIS-associated myoepithelial cells demonstrated decreased staining intensity for one or more myoepithelial markers. The normal localization of myoepithelial cells (flat against the basement membrane, pattern N) was seen in 96% of LCIS, yet 85% of cases had areas with myoepithelial cell cytoplasm oriented perpendicular to the basement membrane (pattern P), and in 30% of cases, myoepithelial cells appeared focally admixed with LCIS cells (pattern C). This study characterizes detailed architectural and immunophenotypic alterations of LCIS-associated myoepithelial cells. The finding of variably diminished staining favors application of several myoepithelial immunostains in clinical practice. The interaction of LCIS with myoepithelial cells, especially in light of the perpendicular and central architectural arrangements, deserves further mechanistic investigation.

© 2016 Elsevier Inc. All rights reserved.

1. Introduction

In normal breast ducts and lobules, myoepithelial cells are situated between the luminal (secretory) epithelium, and the basement membrane. Classic ultrastructural studies demonstrate that they are flattened against the basement membrane with circumferentially oriented nuclei [1]. Furthermore, myoepithelial cells connect with one another through intermediate or gap junctions, to the epithelial cells through

[☆] Disclosures: None.

^{☆☆} A subset of these data was presented in abstract form at the USCAP annual meeting in Boston, MA, on March 24, 2015.

* Corresponding author at: Department of Pathology, Stanford University School of Medicine, L235, 300 Pasteur Drive, Stanford, CA 94305.

E-mail addresses: megant@stanford.edu, mltroxell@yahoo.com (M. Troxell).

desmosomes, and to the basement membrane through hemidesmosomes [2,3]. Myoepithelial cells have important developmental functions, maintain the basement membrane and epithelial cell polarity, and, during lactation, have a contractile function in the process of milk secretion [2–5]. In recent years, the assessment of the presence or absence of myoepithelium using specific immunohistochemical markers has been widely used as a convenient ancillary method to assist in diagnosis of in situ or invasive breast carcinoma, respectively [6].

In 1980, Bussolati et al [1,7] elegantly characterized the relationship of lobular carcinoma in situ (LCIS) and myoepithelial cells using anti-actin immunohistochemistry and electron microscopy. In addition to the commonly recognized “flattened” myoepithelial architecture (“basket-like” pattern A), they also described myoepithelial cells perpendicular to the basement membrane (“offsite disarrangement” pattern B), or myoepithelial cells intermingled with LCIS (“nest-like” pattern C) [7].

Furthermore, recent molecular and immunohistochemical studies have demonstrated that ductal carcinoma in situ (DCIS)-associated myoepithelial cells are different from myoepithelial cells in normal breast and have suggested both physical and paracrine functions in tumor inhibition (or promotion) [2,4,8–12]. Nevertheless, the phenotypic characterization of LCIS-associated myoepithelium remains largely unclear. In this study, we sought to revisit the distribution and characterize the phenotypic features of LCIS-associated myoepithelial cells in a larger series of cases, using a panel of contemporary immunohistochemical markers, including nuclear, cytoplasmic, and dual stains.

2. Materials and methods

2.1. Patients and LCIS specimens

With institutional review board approval, the pathology files of Oregon Health & Science University (2012–2015) were searched for surgical breast resection specimens containing LCIS. Slides were reviewed to select cases with abundant LCIS, many including pagetoid LCIS, and one representative block containing LCIS and normal breast tissue was used for further study. The final study group included 27 specimens from 25 women (2 patients with bilateral LCIS), including 21 classic LCIS and 6 pleomorphic LCIS.

2.2. Immunohistochemical staining

Representative blocks were stained for E-cadherin/smooth muscle myosin heavy chain (SMMHC) dual stain, CK7/p63 dual stain, SMMHC alone, smooth muscle actin (SMA), or calponin using standard methods (Supplementary Table 1) on Benchmark XT or Ultra automated stainers (both Ventana, Tucson, AZ). The Supplementary Data also describe 10 cases immunofluorescently stained for calponin, SMA, and p63.

2.3. Immunohistochemical scoring

In each case, the intensity and distribution of staining in LCIS-associated myoepithelial cells were visually compared with the myoepithelial cells surrounding normal breast tissue on the same slide using the following criteria for all markers: score 1, staining intensity of the myoepithelial cells in LCIS weaker than the normal; score 2, staining intensity in LCIS equals myoepithelial cells in normal breast; and score 3, staining intensity in LCIS stronger than the normal, based on the dominant (most abundant) pattern in LCIS. In addition, architectural patterns were scored, for cytoplasmic markers, pattern N represents normal, flattened peripherally against basement membrane; pattern P, perpendicular to the basement membrane, or “net-like”; and pattern C, central or nest-like. Architectural criteria, for p63, are as follows: pattern N, normal, against basement membrane; pattern P, above basement membrane, especially with 1 layer of epithelial nuclei between p63+ and basement membrane; and pattern C, more than 1 cell layer above the basement membrane. Slides were scored independently by one pathologist and one trainee (M. L. T., Y. W.), and discrepancies were resolved by consensus review.

3. Results

3.1. Patients and LCIS specimens

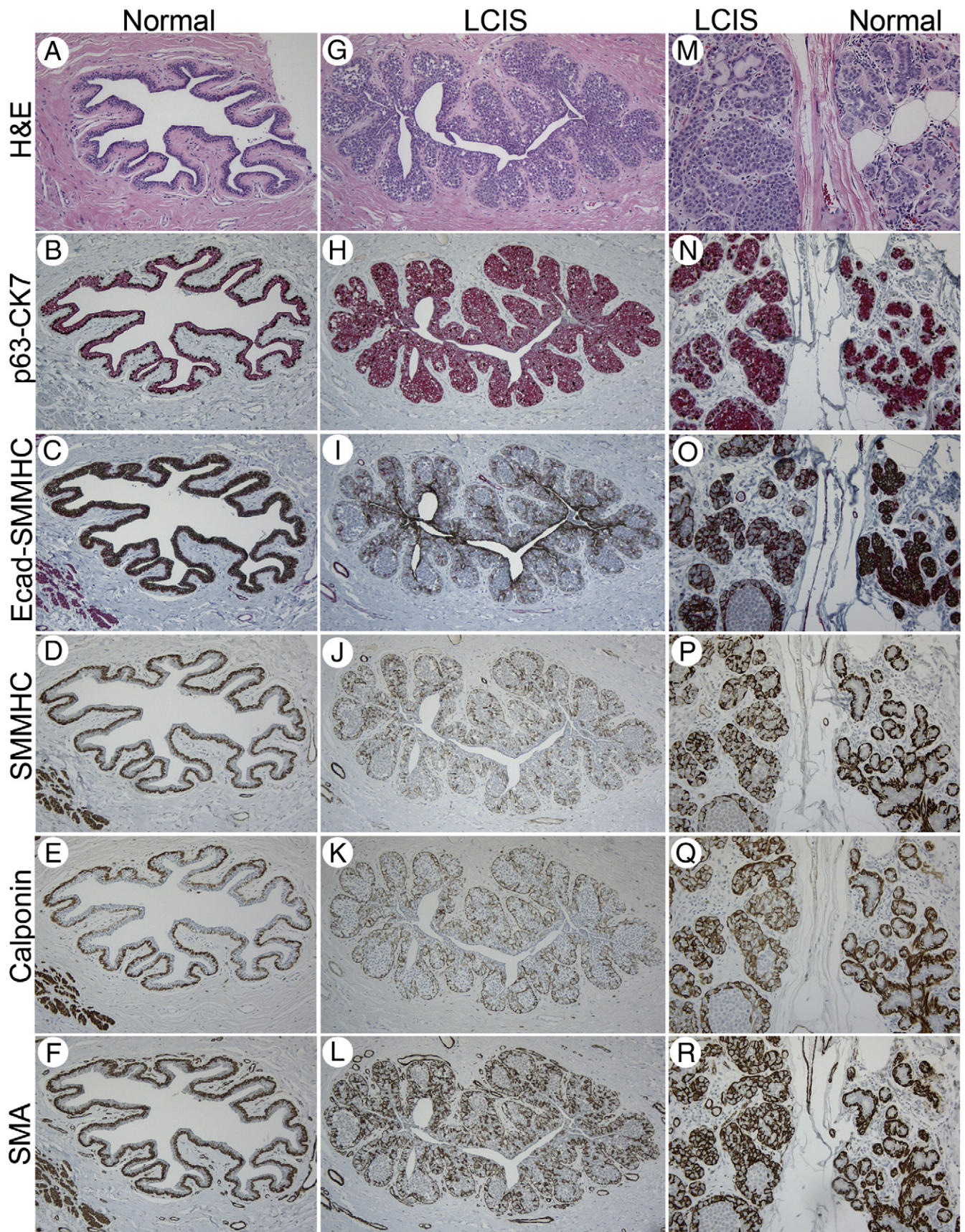
We stained representative blocks from 27 breast resection specimens containing LCIS, from 25 patients (2 bilateral) with a panel of contemporary myoepithelial markers, including dual stains. Cases included 21 classic LCIS and 6 pleomorphic LCIS. Many patients had invasive lobular (19) or ductal (5) carcinoma

Table 1 Staining intensity of LCIS-associated myoepithelial cells compared with myoepithelial cells in accompanying normal breast

Stain	LCIS weaker (pattern 1)	LCIS equal (pattern 2)	LCIS stronger (pattern 3)
Calponin	18/27 (67%)	8/27 (29%)	1/27 (4%)
P63	1/27 (4%)	26/27 (96%)	0
SMA	7/27 (26%)	20/27 (74%)	0
SMMHC	14/27 (52%)	13/27 (48%)	0
SMMHC in dual stain ^a	17/26 (65%)	9/26 (35%)	0

NOTE. LCIS showed variable staining intensity; the dominant (most abundant) pattern was tallied.

^a As compared with SMMHC stained singly, the SMMHC in dual stain was weaker in 7 (28%) of 25, equal in 15 (60%) of 25, and stronger in 3 (12%) of 25.



elsewhere in the specimen (2 patients had both). Four patients did not have invasive carcinoma. Four patients had received neoadjuvant chemotherapy and 1 neoadjuvant endocrine therapy prior to surgery. Patient age ranged from 34 to 85 years (average, 58.3 years).

3.2. Myoepithelial cell phenotypic alterations in LCIS

The staining intensity of calponin, SMMHC, SMA, and p63 in myoepithelial cells associated with LCIS was visually compared with the staining of normal ducts and lobules on the same slide (Table 1 and Fig. 1). In 78% of the cases, LCIS-associated myoepithelial cells demonstrated decreased staining intensity for one or more myoepithelial markers when compared with staining of myoepithelial cells in normal acini and ducts on the same slide. Reduced staining was observed in 67% of LCIS for calponin, 52% for SMMHC, 26% for SMA, and 4% for p63. The intensity of p63 staining was rarely diminished, yet in distended ducts and acini, p63+ nuclei were more widely spaced. Immunofluorescence staining of a subset of cases demonstrated occasional loss of nuclear p63 in myoepithelial cells (see Supplementary Data). Of the cytoplasmic stains, SMA was least often diminished in intensity, but also had the most robust staining of nearby endothelial cells and myofibroblasts (Fig. 1). This cross-reactivity interfered with interpretation in about 10% of cases. SMMHC was evaluated alone and as part of a dual stain using the same primary antibody and retrieval, but different incubation times, different detection chemistry, and different chromagen (Supplementary Table 1). SMMHC in the dual stain was weaker in 28%, equal in 60%, and stronger in 12%, as compared with the single stain. Dual immunofluorescence staining for SMA and calponin demonstrated close colocalization (see Supplementary Data and Supplementary Fig. 1).

3.3. Myoepithelial cell distribution in LCIS

We evaluated the architectural relationships between myoepithelial cells and the accompanying LCIS as demonstrated by single and dual immunostaining. Architectural patterns evaluated are illustrated in Figs. 1 and 2, including the expected normal distribution with myoepithelial cells flattened against the basement membrane and “beneath” the LCIS cells (pattern N, “basket-like arrangement” per Bussolati); myoepithelial cell cytoplasm additionally perpendicular to the basement membrane and interdigitating with LCIS (pattern P, “offside disarrangement” per Bussolati); and centrally

located myoepithelial cells, seemingly intermingled with LCIS (pattern C, “nest-like” after Bussolati) [7]. LCIS in ducts (pagetoid involvement) was particularly illustrative, with less complexity of tangential sectioning as compared with involved lobules. Multiple different arrangements of LCIS and myoepithelial cells were apparent in the same section for most of the cases. All but one case had pattern N (normal, flat); pattern P (perpendicular) was observed in 85% and was the predominant pattern in 26% of LCIS. Pattern C (central, intermingled) was seen focally in 30% of the cases (Table 2).

The addition of the nuclear stain (p63) and dual E-cadherin–SMMHC allowed for further characterization of myoepithelial cell architecture in LCIS. In normal ducts and acini, p63+ myoepithelial cell nuclei are situated on or very close to the basement membrane (Figs. 1 and 2, pattern N). However, in LCIS, the p63+ myoepithelial cell nuclei were identified one cell layer above the basement membrane (Figs. 2 [patterns P and C], 3A and 4A and D). This was seen at least focally in 92.5% of cases and in 5 of 6 examples of pleomorphic LCIS. In one case of LCIS in a nipple duct, the E-cadherin (brown)–SMMHC (red) dual stain illustrated myoepithelial cells “bridging” or stretched from the basement membrane to the overlying layer of residual E-cadherin+ ductal epithelial cells, between LCIS cells (Fig. 3D–F). Furthermore, the dual stain also better highlighted myoepithelial cells capping the outermost layer of LCIS, with myoepithelial cell cytoplasm parallel to the basement membrane, but one cell layer above it (Figs. 3B, D, and G and 4B and F). These architectural patterns were especially obvious in cases of pleomorphic LCIS, as the outermost nuclear layer had grade 3 nuclei of pleomorphic LCIS and was readily distinguished from myoepithelial nuclei, without cytoplasmic staining for any of the tested markers, yet these cells were surrounded by E-cadherin+ SMMHC+ myoepithelial cells (Fig. 4A–G).

3.4. Myoepithelial continuity

These different architectural arrangements of myoepithelial cells can result in discontinuities in the ring of myoepithelial cytoplasm surrounding LCIS. Discontinuities varied considerably across myoepithelial immunostains. However, in 13 cases, the same discontinuities were seen in all of the cytoplasmic stains; in 3 cases, the breaks in the continuous ring were rare and small, on the order of single-cell size. In 9 cases, there were corresponding gaps in the sequence of p63+ nuclei either at the basement membrane or one layer removed. In one case, large areas of LCIS were virtually devoid of myoepithelial

Fig. 1 Myoepithelial cell staining in normal breast compared with LCIS. A–F, Myoepithelial cell staining in a normal nipple duct, patient 4, serial sections. Smooth muscle bundles (lower left of each panel) are stained strongly with actin machinery cytoplasmic markers. SMMHC and calponin stain endothelial cells weakly, whereas SMA stains endothelium strongly (right and bottom). G–L, myoepithelial cell staining in LCIS involving a nipple duct, adjacent to the duct shown at left, patient 4. Note the different distribution and generally weaker staining in LCIS. M–R, Myoepithelial cells in normal acini (right of each panel) juxtaposed to LCIS (left of each panel), serial sections from patient 18–L. The intensity of staining is similar, yet myoepithelial cells have a different distribution in acini involved by LCIS, admixed with and enveloping the outermost layer of LCIS (see Figs. 2–5). Original magnifications $\times 100$ (A–L) and $\times 200$ (M–R). For dual stains: p63 (brown)–CK7 (red), E-cadherin (brown)–SMMHC (red).

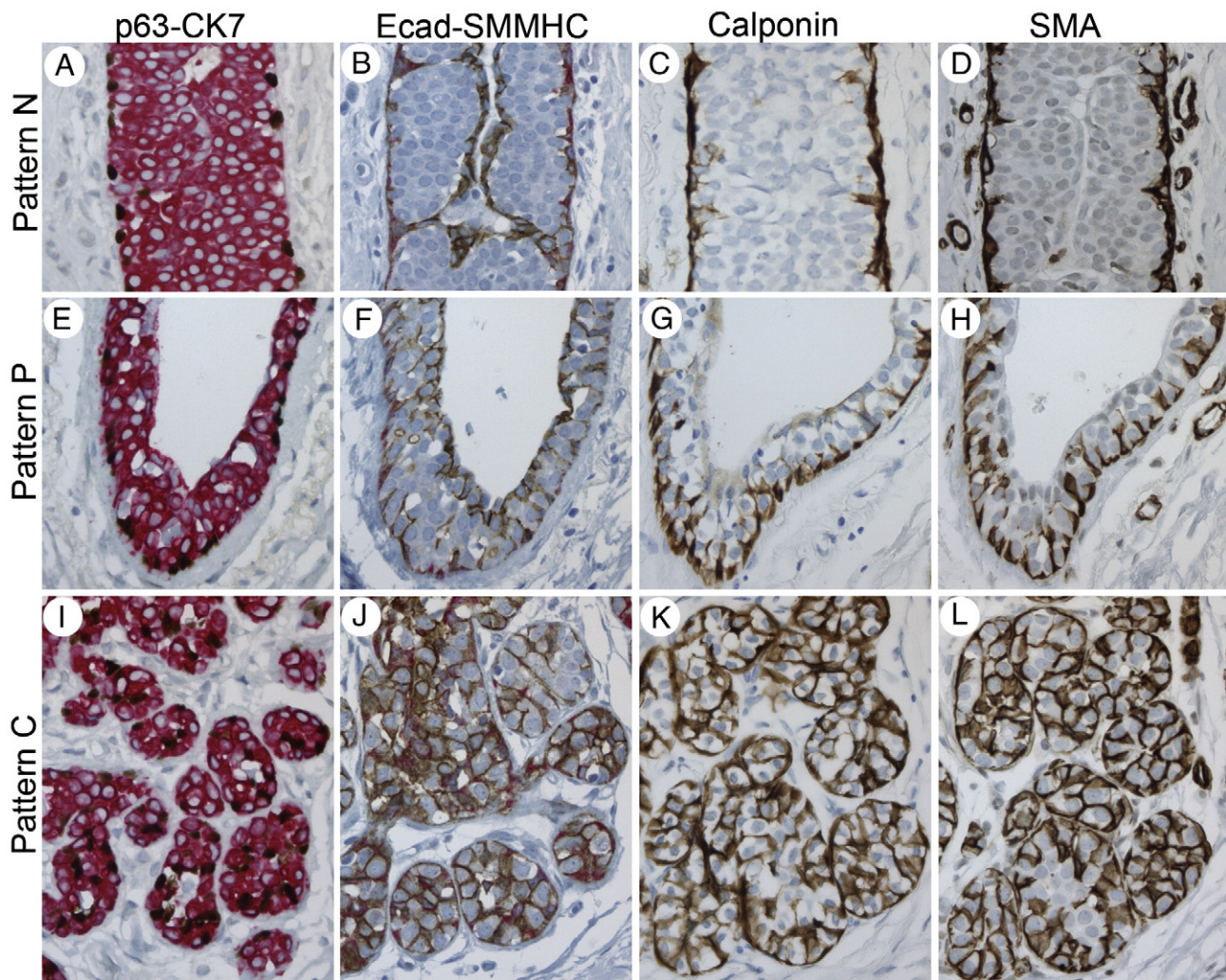


Fig. 2 Architectural relationships of myoepithelial cells and LCIS: patterns. A–D, Pattern N (normal). Myoepithelial cells lie flat on the basement membrane and form a continuous layer “beneath” the LCIS. Serial sections from patient 12, pagetoid LCIS in a duct. E–H, Pattern P (perpendicular). Myoepithelial cell cytoplasm is seen perpendicular to the basement membrane and interdigitates between LCIS cells in the outermost cell layer. The continuous ring of myoepithelial cell cytoplasm around the ductal space is essentially maintained. In this example, p63+ myoepithelial nuclei are situated against the basement membrane. Serial sections from patient 8, pagetoid LCIS. I–L, Pattern C (central, admixed). Myoepithelial cells are seen centrally within these acini, intermixed with LCIS. Note that the p63+ myoepithelial nuclei are often at least 1 cell layer offset from basement membrane. Serial sections from patient 8. With the E-cadherin (brown)–SMMHC (red) dual stain, myoepithelial cells stain red–cytoplasmic plus brown–membrane, whereas ductal epithelial cells stain brown–cell membrane, and LCIS is negative for both. Original magnifications $\times 400$. For dual stains: p63 (brown)–CK7 (red), E-cadherin (brown)–SMMHC (red).

cells (Supplementary Fig. S2). In the 4 cases without accompanying invasive carcinoma, myoepithelial staining gaps were seen in 2, and each of the architectural patterns of myoepithelial cells was observed (N, P, C), in these cases without invasion. However, the number of cases without invasive carcinoma in this study is too small to draw further comparisons.

4. Discussion

Breast myoepithelial cells have recently gained attention as having a potential role in invasion and tumor suppression,

largely studied in the context of DCIS [2,4,8–12]. Hilson and colleagues recently demonstrated decreased myoepithelial cell protein staining/expression in DCIS, with differences by antibody stain and grade of DCIS [9]. In a separate study, they investigated benign sclerosing lesions and suggested lesion-specific differences [13], yet LCIS has not been studied in this fashion. Although myoepithelial cell immunostains are rarely needed to distinguish LCIS from classic patterns of invasive lobular carcinoma with “single-file” cell architecture, certain situations require additional studies, such as LCIS involving sclerosing adenosis or other sclerosing lesions, especially to differentiate from the trabecular, alveolar, or even solid architectural patterns of invasive lobular carcinoma. Furthermore,

Table 2 Architectural relationships of LCIS and myoepithelial cells

Pattern	All LCIS cases		Pleomorphic LCIS	
	Dominant pattern	Cases with any	Dominant pattern	Cases with any
N: normal, flat	20/27 (74%)	26/27 (96%)	4/6 (67%)	5/6 (83%)
P: perpendicular to basement membrane	7/27 (26%)	23/27 (85%)	2/6 (33%)	6/6 (100%)
C: central, intermingled	0	8/27 (30%)	0	2/6 (33%)

combination or concurrent keratin stains can also help reveal occult invasive carcinoma in certain instances. We found that areas involved by LCIS frequently had diminished intensity

of myoepithelial staining when compared with normal breast, with one or several traditional myoepithelial cell cytoplasmic immunomarkers (Table 1). p63, a nuclear transcription factor,

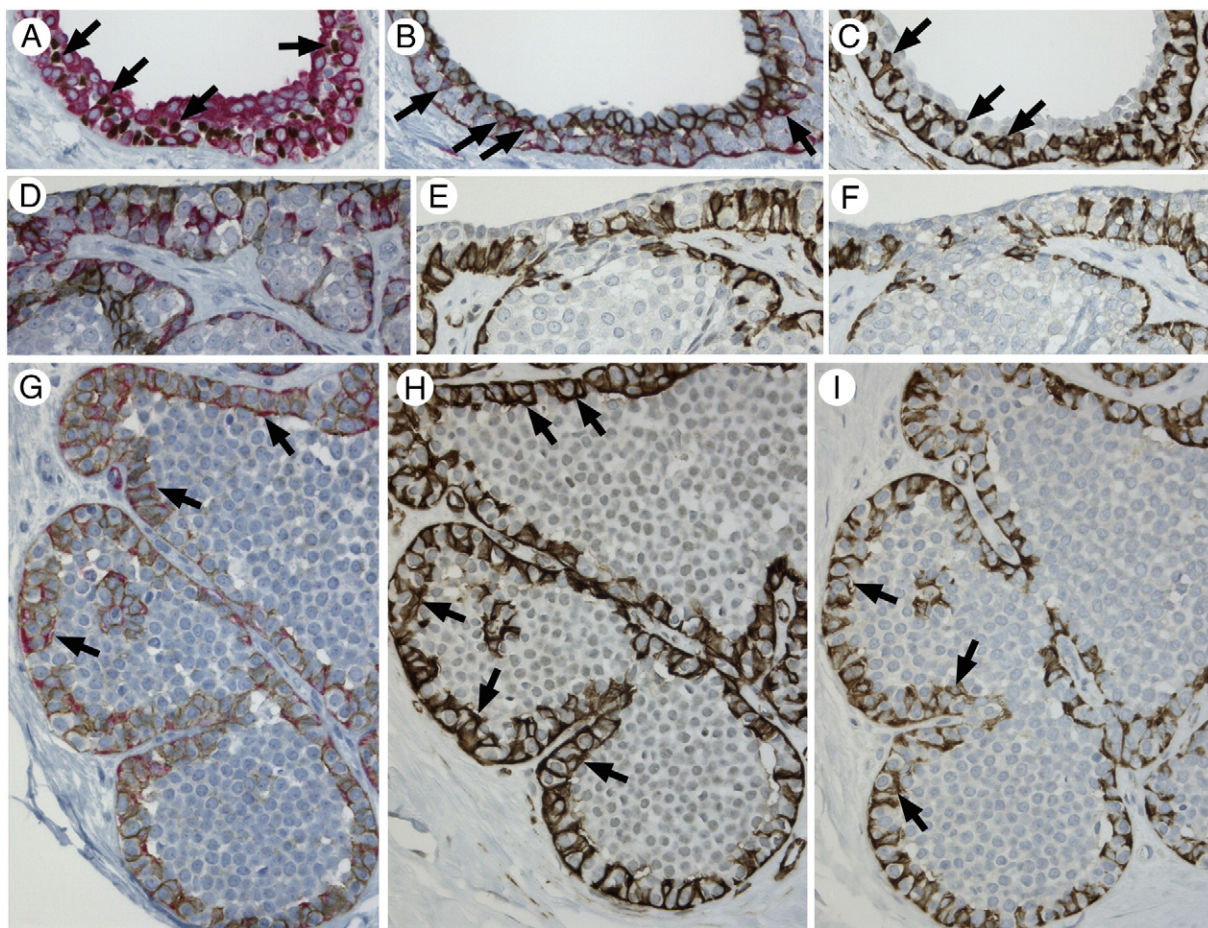


Fig. 3 Myoepithelial cells in LCIS. A-C, LCIS with myoepithelial cells perpendicular to the basement membrane (pattern P) and myoepithelial nuclei one to several cell layers above the basement membrane, serial sections patient 25, pleomorphic LCIS. A, CK7 (red)–p63 (brown) dual stain; note: brown p63+ myoepithelial cell nuclei intermingle with LCIS (examples: arrows). B, E-cadherin (brown)–SMMHC (red) dual stain. Red myoepithelial cell cytoplasm is seen between negative LCIS cells. Smaller myoepithelial cell nuclei, surrounded by SMMHC+ red cytoplasm, are seen juxtaposed to the inner ductal cell layer (examples: arrows). C, SMA immunohistochemistry shows myoepithelial cell cytoplasm connecting the basement membrane to the myoepithelial cell nuclei (myoepithelial cell nuclei; examples, arrows). SMA also demonstrates the integrity of the circumferential myoepithelial cell layer against the basement membrane. D-F, LCIS with pagetoid pattern in a nipple duct; myoepithelial cells “bridge” between basement membrane and ductal epithelial cells; serial sections from patient 13. D, E-cadherin (brown)–SMMHC (red) dual stain. E, Red myoepithelial cell cytoplasm SMA stain; brown myoepithelial cell cytoplasm. F, SMMHC stain; brown myoepithelial cell cytoplasm. G-I, LCIS involving distended spaces with myoepithelial cells perpendicular to the basement membrane at the outermost layer of LCIS (pattern P), and sometimes encircling LCIS (arrows). Serial sections from patient 15. G, E-cadherin (brown)–SMMHC (red) dual stain. H, SMA; arrows point to examples of myoepithelial cells encircling LCIS. I, SMMHC; arrows point to some of the small myoepithelial cell nuclei, where they are displaced above the basement membrane. Original magnifications $\times 400$.

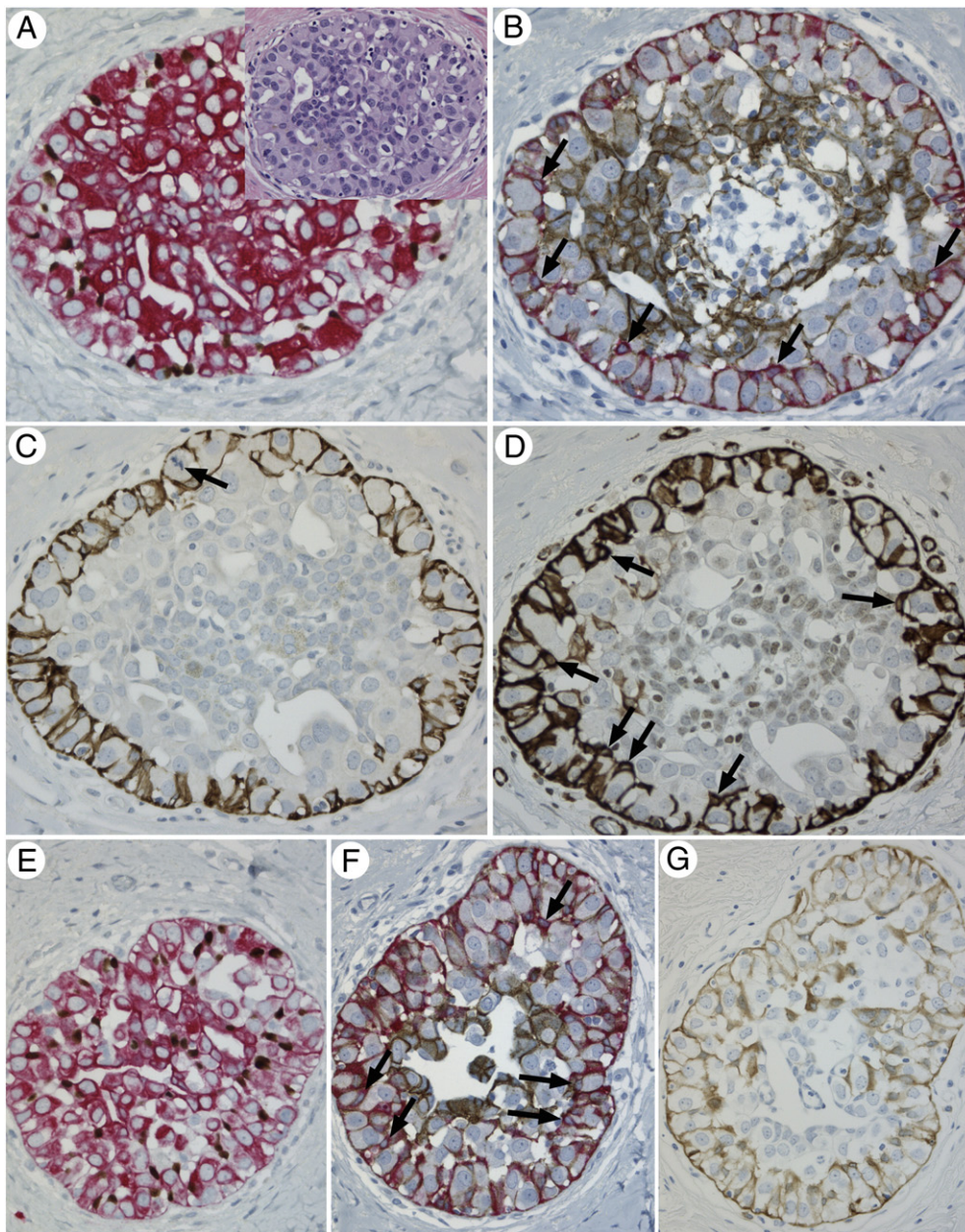


Fig. 4 Myoepithelial cells in pleomorphic LCIS. A-D, A ductal space involved by pleomorphic LCIS with myoepithelial patterns P and C. Serial sections from patient 23, after neoendocrine therapy. A, CK7 (red)–p63 (brown) dual stain. Many p63+ nuclei are situated above the basement membrane. Inset, hematoxylin and eosin. B, E-cadherin (brown)–SMMHC (red) dual stain; small myoepithelial nuclei offset from the basement membrane are connected by red-staining SMMHC+ cytoplasm (arrows: examples). Numerous remnant ductal cells have brown E-cadherin+ membranes, center. C, SMMHC; in the left side of the field, the outermost layer of pleomorphic LCIS cells is completely encircled by myoepithelial cell cytoplasm. Arrow denotes mitotic figure in LCIS. D, SMA; arrows show some of the myoepithelial cell nuclei. Note that the myoepithelial cell layer remains peripherally continuous in cytoplasmic stains. E-G, Pleomorphic LCIS with myoepithelial cells intermixed (pattern C). Serial sections from patient 23. E, CK7 (red)–p63 (brown) dual stain shows p63+ myoepithelial cell nuclei scattered throughout various layers of the proliferation. F, E-cadherin (brown)–SMMHC (red) dual stain; several small myoepithelial cell nuclei are shown by arrows. Myoepithelial cell cytoplasm (red) interdigitates with pleomorphic LCIS. Also note unbroken peripheral myoepithelial staining. E-cadherin+ ductal cells are present centrally. G, Calponin stains myoepithelial cells weakly and shows the same architectural relationships. Original magnifications $\times 400$.

seldom exhibited diminished staining intensity in LCIS (Table 1), but occasional p63-negative myoepithelial nuclei were observed by immunofluorescence staining (see Supplementary Data) [12]. The loss of p63 staining may represent phenotypic alteration of

LCIS–myoepithelial cells, because the cytoplasmic myoepithelial markers SMA and/or calponin are intact. Similar to the findings of Hilson et al [9,13] for DCIS, we found that SMA was the most robust of the actin-contractile machinery cytoplasmic

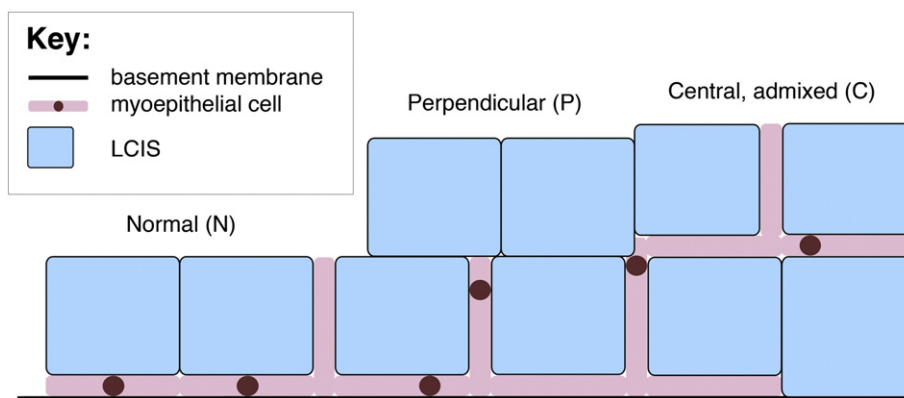


Fig. 5 Myoepithelial cells in LCIS: schematic. Architectural relationships of myoepithelial cells observed in LCIS. Brown circle indicates myoepithelial cell nucleus. (For interpretation of the references to color in this figure legend, the reader is referred to the web version of this article.)

stains that we tested in LCIS. However, SMA also stained endothelial cells and myofibroblasts more prominently than SMMHC and calponin [9]. This SMA reactivity seldom interfered with interpretation of myoepithelial staining (data not shown); nevertheless, SMA is no longer a first-line myoepithelial cell marker in many laboratories [9]. The variable performance of these markers in LCIS supports a panel approach, in which more than one stain is applied (in our hands, p63 and one of the cytoplasmic markers), as has been encouraged for DCIS [9].

In the 1980s, Bussolati et al [1,7] elegantly described different architectural patterns of myoepithelial cells in LCIS lesions, using electron microscopy and a single actin immunostain. They studied 4 LCIS lesions by electron microscopy, actin immunofluorescence, and immunohistochemistry, and another 13 LCIS by actin immunohistochemistry on formalin-fixed, paraffin-embedded tissue [1,7]. We applied a panel of contemporary immunostains, including nuclear and dual stains, to characterize myoepithelial architecture in detail in a larger series of LCIS (Fig. 5). We found architectural alterations, including myoepithelial cells perpendicular to the basement membrane, or admixed with LCIS (patterns P, C) in 85% of LCIS cases studied. Furthermore, the addition of the p63 nuclear stain revealed that myoepithelial nuclei were frequently displaced one cell layer above the basement membrane (Figs. 2–5). In some cases, myoepithelial cells capped the most peripheral layer of LCIS (Figs. 3–5). Anecdotally, these architectural arrangements are relatively unique to LCIS and, when abundant, are distinctive even at scanning magnification (patterns P and C, Fig. 1). These architectural observations suggest unique interactions between LCIS and myoepithelial cells. The function, cellular mechanism, and implications of such LCIS-myoeplithelial interactions deserve further study.

Despite these aberrations, the myoepithelial cells generally maintained their continuous circumferential organization between the basement membrane and LCIS. In almost half of the cases, small gaps in myoepithelial continuity were noted on careful examination, although the gaps varied considerably by stain and by case, again favoring the panel approach [9,13]. One case exhibited widespread loss of myoepithelial cells in

LCIS (Supplementary Fig. S2). This case shares some similarities to the cases illustrated by Zhang et al [14]. They reported segmental gaps in myoepithelial labeling in 3 (1.7%) of 175 tested cases. Their 3 cases with morphologically apparent myoepithelial layer but lack of reactivity with 9 different myoepithelial antibodies included 1 columnar cell hyperplasia and 2 DCIS [14]. Their study included an unspecified number of LCIS samples, in which loss of myoepithelial staining was not reported [14]. Our cohort was too small to draw meaningful associations between myoepithelial continuity and presence or absence of an invasive component.

In conclusion, we have characterized in detail immunophenotypic and architectural alterations in LCIS-associated myoepithelial cells. We demonstrate not only changes in staining intensity as was previously illustrated for DCIS and sclerosing lesions, but also unique relationships of myoepithelial and epithelial cells in ducts and acini involved by LCIS. The cell-cell interactions behind the unique LCIS-myoeplithelial cell architecture and their significance in terms of cancer progression are topics for future study. In terms of diagnostic practice, our findings support the application of a multistain panel in assessing invasion in the context of LCIS.

Supplementary data

Supplementary data to this article can be found online at <http://dx.doi.org/10.1016/j.humpath.2016.05.003>.

Acknowledgments

The authors wish to acknowledge expert immunohistotechnical support from Linh Matsumura and the graphical expertise of Jared Olivas. The authors also acknowledge Dr Lisa Coussens (Oregon Health & Science University, Portland) for support with immunofluorescent image scanning on Ariol Scanscope.

References

- [1] Bussolati G, Botto Micca FB, Eusebi V, Betts CM. Myoepithelial cells in lobular carcinoma in situ of the breast: a parallel immunocytochemical and ultrastructural study. *Ultrastruct Pathol* 1981;2:219-30.
- [2] Deugnier MA, Teulière J, Faraldo MM, Thiery JP, Glukhova MA. The importance of being a myoepithelial cell. *Breast Cancer Res* 2002;4:224-30.
- [3] Lakhani SR, O'Hare MJ. The mammary myoepithelial cell—Cinderella or ugly sister? *Breast Cancer Res* 2001;3:1-4.
- [4] Adriance MC, Inman JL, Petersen OW, Bissell MJ. Myoepithelial cells: good fences make good neighbors. *Breast Cancer Res* 2005;7:190-7.
- [5] Polyak K, Hu M. Do myoepithelial cells hold the key for breast tumor progression? *J Mammary Gland Biol Neoplasia* 2005;10:231-47.
- [6] Lerwill MF. Current practical applications of diagnostic immunohistochemistry in breast pathology. *Am J Surg Pathol* 2004;28:1076-91.
- [7] Bussolati G. Actin-rich (myoepithelial) cells in lobular carcinoma in situ of the breast. *Virchows Arch B Cell Pathol Incl Mol Pathol* 1980;32:165-76.
- [8] Man YG, Tai L, Barner R, et al. Cell clusters overlying focally disrupted mammary myoepithelial cell layers and adjacent cells within the same duct display different immunohistochemical and genetic features: implications for tumor progression and invasion. *Breast Cancer Res* 2003;5:R231-41.
- [9] Hilson JB, Schnitt SJ, Collins LC. Phenotypic alterations in ductal carcinoma in situ—associated myoepithelial cells: biologic and diagnostic implications. *Am J Surg Pathol* 2009;33:227-32.
- [10] Barsky SH, Karlin NJ. Mechanisms of disease: breast tumor pathogenesis and the role of the myoepithelial cell. *Nat Clin Pract Oncol* 2006;3:138-51.
- [11] Allinen M, Beroukhi R, Cai L, et al. Molecular characterization of the tumor microenvironment in breast cancer. *Cancer Cell* 2004;6:17-32.
- [12] Russell TD, Jindal S, Agunbiade S, et al. Myoepithelial cell differentiation markers in ductal carcinoma in situ progression. *Am J Pathol* 2015;185:3076-89.
- [13] Hilson JB, Schnitt SJ, Collins LC. Phenotypic alterations in myoepithelial cells associated with benign sclerosing lesions of the breast. *Am J Surg Pathol* 2010;34:896-900.
- [14] Zhang RR, Man YG, Vang R, et al. A subset of morphologically distinct mammary myoepithelial cells lacks corresponding immunophenotypic markers. *Breast Cancer Res* 2003;5:R151-6.